

Article

Core/CdS Quantum Dot/Shell Mesoporous Solar Cells with Improved Stability and Efficiency Using an Amorphous TiO Coating

Menny Shalom, Snir Dor, Sven Ru#hle, Larissa Grinis, and Arie Zaban

J. Phys. Chem. C, **2009**, 113 (9), 3895-3898 • DOI: 10.1021/jp8108682 • Publication Date (Web): 06 February 2009

Downloaded from <http://pubs.acs.org> on May 18, 2009

More About This Article

Additional resources and features associated with this article are available within the HTML version:

- Supporting Information
- Access to high resolution figures
- Links to articles and content related to this article
- Copyright permission to reproduce figures and/or text from this article

[View the Full Text HTML](#)

Core/CdS Quantum Dot/Shell Mesoporous Solar Cells with Improved Stability and Efficiency Using an Amorphous TiO₂ Coating

Menny Shalom, Snir Dor, Sven Rühle, Larissa Grinis, and Arie Zaban*

Department of Chemistry, Bar Ilan University, Ramat Gan 52900, Israel

Received: December 10, 2008; Revised Manuscript Received: January 5, 2009

Here we present a CdS quantum dot sensitized solar cell based on a mesoporous TiO₂ film with remarkable stability using I⁻/I₃⁻ electrolyte. Chemical Bath Deposition (CBD) was used to deposit the CdS quantum dots within the porous network. We show that a thin coating of the QD sensitized film with an amorphous TiO₂ layer strongly improves the performance and photostability of the solar cell. We propose that the coating passivates QD surface states which act as hole traps and are responsible for photodegradation of the device. In addition, this coating decreases the recombination of electrons from the CdS quantum dots and the mesoporous TiO₂ into the electrolyte solution. We obtain a significant improvement of all cell parameters resulting in a total light to electric power conversion efficiency of 1.24%.

Introduction

Dye sensitized solar cells (DSSC) and quantum dot (QD) sensitized solar cells are extensively studied because they are potential low cost alternatives to existing silicon cells. DSSCs are based on a several micrometer thick mesoporous TiO₂ film consisting of anatase nanocrystals, deposited onto a conducting transparent substrate (TCO) and covered with a monolayer of dye. The pores are filled with a redox electrolyte and the circuit is closed by a Pt coated counter electrode. Under illumination photons are absorbed by the dye, which injects an electron from the excited state into the conduction band (CB) of the TiO₂, while the oxidized dye is recharged by the redox electrolyte. Energy conversion efficiencies around 11% have been achieved using a ruthenium complex as a sensitizer together with a I⁻/I₃⁻ redox electrolyte.^{1,2} Though other redox couples have been investigated, no competitive couple has been found, emphasizing the unique properties of I⁻/I₃⁻ in DSSCs. Alternative to the ruthenium complex, semiconductor QDs such as CdS,^{3–7} CdSe,^{8–10} PbS,¹¹ InAs,¹² and InP¹³ have been used as sensitizers that absorb light in the visible region. QDs have a higher absorption coefficient than most organometallic or organic dyes, thus allowing the use of thinner mesoporous electrodes compared to dye sensitized ones, which is highly desired for solid state devices, where the liquid electrolyte is replaced by a solid state hole conductor. Due to size confinement, the absorption spectrum of QDs can be tailored,¹⁴ which is of particular importance when QD sensitized solar cells are used as building blocks for multijunction third generation photovoltaic devices. However, in spite of its great potential, the solar conversion efficiency of inorganic QD sensitized solar cells has reached only around 2.9% at present.^{15–18}

One reason for the rather moderate conversion efficiency of QD sensitized solar cells is the presence of surface states in the QDs, which act as recombination centers and can lead to degradation. Photoexcited electrons can be trapped in surface states and injection into the TiO₂ CB is unfavorable if the surface state is energetically located below the TiO₂ CB edge. Trapped electrons can recombine either with a hole in the QD or they are captured by the oxidized species of the redox electrolyte.

Trapped holes on the contrary can recombine with excited electrons in the QD or with electrons from the TiO₂. In addition, accumulation of holes inside surface states of the CdS QDs can result in degradation and photoinstability of the cell.^{19,20} This is of particular importance if the I⁻/I₃⁻ redox electrolyte is used, which is very corrosive. Blocking trap states by coating the particles with thin layers of a wide band gap material can lead to a drastic enhancement of the photostability.²¹

Deposition of QDs onto the mesoporous TiO₂ films often results in a noncontinuous layer with uncovered TiO₂ areas, which are in contact with the redox-electrolyte.^{3,6} Under solar cell operation, electrons injected into the TiO₂ can recombine with the electrolyte via the uncovered areas, which reduces the cell efficiency. Coating of the uncovered TiO₂ prevents contact of the electrolyte with the TiO₂ particles, thus decreasing the reaction rate via this recombination path.²²

In this work, CdS QDs were deposited by chemical bath deposition (CBD) as a photosensitizer onto the surface of interconnected TiO₂ nanocrystals forming a mesoporous film (core material). We show that the deposition of a thin amorphous TiO₂ shell around the QD sensitized electrode improves both, the solar cell performance and its photostability. We propose that the amorphous TiO₂ shell passivates QD surface states, which act as hole traps and are responsible for photodegradation of the device. In addition, this coating decreases the recombination of electrons from the CdS quantum dots and the mesoporous TiO₂ into the electrolyte solution. The protective shell enabled us to use the I⁻/I₃⁻ redox couple which resulted in a higher open circuit voltage and fill factor compared to cells using polysulfide electrolyte which is commonly used in conjunction with CdS absorbers.^{17,18,20} A light to electric power conversion efficiency η of 1.24% was achieved with the coated electrodes.

Experimental Section

Mesoporous TiO₂ films were prepared by electrophoretic deposition (EPD)²³ of Degussa P25 particles with an average diameter of 25 nm onto a fluorine-doped tin oxide (FTO) covered glass substrates (Pilkington TEC 15) with 15 Ω /square sheet resistance. Films were deposited in two consecutive cycles for 30 s at a constant current density of 0.4 mA/cm² (which

* Corresponding author: E-mail: zabana@mail.biu.ac.il.

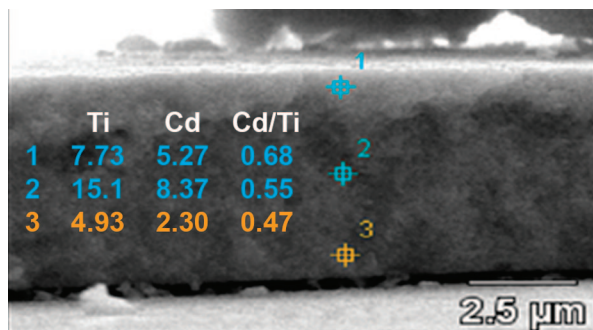


Figure 1. Cross-section SEM image of the CdS QD sensitized mesoporous TiO₂ film showing the TCO substrate at the bottom. The Cd to Ti ratio was measured at three different distances from the TCO substrate.

corresponded to ~ 70 V at an electrode distance of 50 mm) and dried at 120 °C for ~ 5 min in between the cycles. Following the EPD process all the electrodes were dried in air at 150 °C for 30 min, pressed under 800 kg/cm² using a hydraulic press, and sintered at 550 °C for 1 hr. For CdS QDs deposition, the electrodes were immersed in a mixture of 2.35 mL of 0.5 M CdSO₄ and 2.65 mL of 0.7 M potassium nitrilotriacetate (K₃NTA) at pH 8.5 adjusted by 10% KOH. This solution was mixed with 4.25 mL of 0.4 M thiourea and then diluted with 7.55 mL of distilled water. Finally, the pH was readjusted to pH 11 using again 10% KOH. After the electrode was immersed into the solution, it was heated up to 80 °C for two hours,^{24,25} resulting in CdS coating of the mesoporous TiO₂ electrode. The final step involved thin TiO₂ coating of the CdS-sensitized mesoporous TiO₂ electrode by electrophoretic deposition of stabilized TiO₂ precursor (Ti(O₂C₃H₇)₄) followed by oxidation in air.²⁶ Mild heat treatment of the coated electrodes at 80 °C for 10 min was used to stabilize the amorphous TiO₂ shell.

The thickness of the mesoporous electrode was measured with a profilometer (Surftest SV 500, Mitutoyo Co). An I⁻/I₃⁻ redox electrolyte was used in the CdS QDs sensitized solar cells consisting of 0.1 M lithium iodide, 0.05 M iodine, 0.6 M 1-propyl-2,3-dimethylimidazolium iodide, and 0.5 M 4-*tert*-butylpyridine dissolved in propylenecarbonate. A Pt-coated FTO glass was used as a counterelectrode. Photocurrent–voltage characteristics were performed with an Eco-Chemie Potentiostat using a scan rate of 10 mV/s. A 250 W xenon arc lamp (Oriol) calibrated to 100 mW/cm² (AM 1.5 spectrum) served as a light source. The illuminated area of the cell was 0.64 cm². To measure the photocurrent versus time the illumination was turned on and off using an automatic shutter.

Results and Discussion

A cross-section scanning electron microscope (SEM) image of the CdS QD sensitized electrode is shown in Figure 1, together with EDS data, recorded at three different distances from the TCO substrate. The results show the presence of CdS QDs throughout the mesoporous electrode. However, the decreasing Cd to Ti ratio toward the TCO reveals the deposition of smaller amounts of CdS QDs deeper inside the electrode. This phenomenon defines an optimal thickness for the mesoporous TiO₂ electrode. Larger amounts of CdS can be deposited on thicker electrodes thus increasing the overall optical density, but at the same time it leads to lower coverage, especially near the conducting substrate resulting in higher recombination currents. We present the impact of the thin amorphous TiO₂ shell around the CdS sensitized nanocrystalline TiO₂ network

on the recombination paths inside the electrode. For the system reported here, the optimal mesoporous TiO₂ film thickness was 5.5 μm.

The performance of CdS QD sensitized solar cells is shown in Figure 2. The I–V characteristics under illumination and in the dark of two CdS sensitized solar cells with and without coated amorphous TiO₂ shell using I⁻/I₃⁻ as a redox electrolyte are compared in Figure 2a and b, respectively. A strong effect of the amorphous coating is observed both in the dark and under illumination. Under illumination (Figure 2a), the performance of the cell containing the coated electrode is significantly higher due to an increase of the short circuit current density J_{sc} , the open circuit voltage V_{oc} , and the fill factor. Table 1 summarizes the parameters for the first I–V scan showing a 10-fold increase of the conversion efficiency achieved by the coating. The measurements were recorded at a scan rate of 10 mV/s after 15 s of illumination at short circuit. The amorphous TiO₂ coated electrode showed good reproducibility in consecutive I–V scans, while the performance of the uncoated system decreased with each scan. In the dark, electron transfer from the coated electrode into the electrolyte at forward bias is significantly reduced compared to the uncoated electrode (Figure 2b). This indicates that the amorphous TiO₂ shell reduces the recombination of electrons from the mesoporous electrode into the redox electrolyte.

To test the photostability of both coated and noncoated electrodes in the presence of an I⁻/I₃⁻ electrolyte, the short circuit current was measured versus time. Therefore, the illumination was periodically turned on and off with an interval length of 12 s using an automatic shutter. Figure 2c shows the results for both electrodes, where the measurement started under dark condition. The photocurrent of the noncoated electrode already decreased during the second illumination cycle and decreased further with each following cycle. In contrast, the amorphous TiO₂ coated electrode showed a stable photocurrent. For noncoated electrodes the decrease in photocurrent upon illumination was associated with the bleaching of CdS QDs, which is a result of CdS photodegradation in the presence of I⁻/I₃⁻.^{19,20,27} The coating prevents the degradation of the CdS QDs, thus increasing the photostability of the cell.

The short circuit current as a function of the illumination intensity is shown in Figure 2d, where the photocurrent was first measured at the highest light intensity before it was stepwise decreased using neutral density filters. A linear behavior is observed for both electrodes at light intensities below 0.5 suns (50 mW cm⁻²). At higher intensities the photocurrent of the noncoated electrode saturates while the coated system shows a linear behavior over the entire intensity range. The nonlinear behavior of the noncoated electrode, also observed by others,²⁸ indicates increasing recombination rates at light intensities approaching 1 sun.

Figure 3 shows a schematic drawing of the mesoporous TiO₂ film deposited onto a transparent conducting substrate, sensitized with the CdS QDs together with an energy band diagram. Figure 3a schematically shows the film without the amorphous TiO₂ shell. A decreasing CdS coverage toward the TCO substrate is depicted, consistent with EDS data (Figure 1). Five recombination paths in the uncoated system are shown in Figure 3a and in energy band diagrams in Figure 3b and c: (1) trap assisted electron–hole recombination within the QD, (2) injection of trapped electrons from the CdS QD into the electrolyte, (3) injection of electrons from the excited CdS QD state into the electrolyte, (4) recombination of electrons in the TiO₂ nanoparticles with trapped holes in the QDs, and (5) electron loss from TiO₂ nanoparticles into the electrolyte.

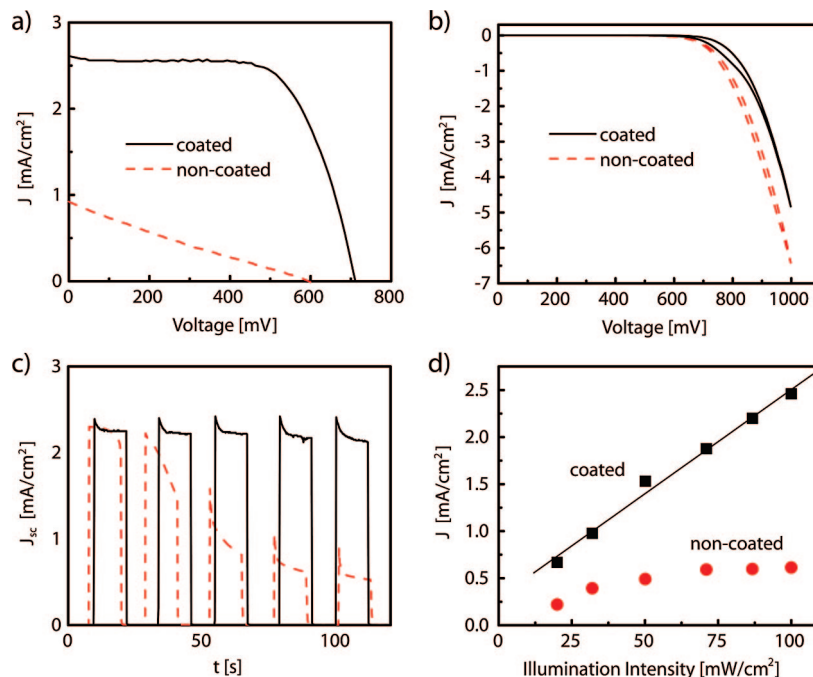


Figure 2. Characterization of the CdS-QDs sensitized TiO₂ solar cells with (solid) and without amorphous TiO₂ coating (dashed). (a) I–V measurement under illumination of one sun (100 mW cm⁻²) and (b) under dark conditions. (c) Short circuit current density as a function of time using periodic illumination intervals (12 s interval length). (d) Photocurrent density as a function of the illumination intensity for the coated (squares) and noncoated electrode (circles).

TABLE 1: Solar Cell Parameters of the CdS Quantum Dot Sensitized Mesoporous TiO₂ Electrode With and Without Amorphous TiO₂ Coating

	J_{sc} [mA cm ⁻²]	V_{oc} [mV]	fill factor [%]	η [%]
amorphous TiO ₂ coated	2.61	715	66	1.24
noncoated	0.92	595	23	0.13

Figure 3d shows the CdS sensitized electrode with a very thin amorphous TiO₂ shell coated around the QD sensitized electrode. The amorphous coating passivates the CdS quantum dot surface by decreasing the trap density and prevents direct contact with the redox electrolyte, which both reduces recombination. The I–V measurements in Figure 2b show that the thin amorphous TiO₂ layer blocks electron transfer from the nanocrystalline TiO₂ and/or the QDs into the electrolyte.¹⁹ Marin and co-workers determined the band gap of amorphous TiO₂ (dc magnetron sputtered) to be in the range of 3.3–3.5 eV,²⁹ which is larger than the bandgap of crystalline anatase. Though the position of the conduction and valence band edge (E_{CB} and E_{VB} , respectively) are not exactly known the smaller dark current of the coated electrode indicates that the E_{CB} of amorphous TiO₂ is located closer to the vacuum level compared to nanocrystalline TiO₂ and acts as a barrier layer for electron transfer from the nanocrystalline TiO₂ core into the electrolyte. The improved solar cell performance with the coating suggests that the amorphous TiO₂ shell does not significantly block hole injection from the QDs into the electrolyte, indicating that the E_{VB} of the coating is located close to the QD ground-state level. Assuming this, the E_{CB} of the amorphous TiO₂ shell is located sufficiently close to the vacuum level to create also a barrier for electron injection from the excited CdS QDs into electrolyte.

The amorphous coating furthermore protects the CdS QDs from the very corrosive I⁻/I₃⁻ redox couple, which showed a better performance compared to other electrolytes such as polysulfide. Degradation, which can stem from chemical reaction

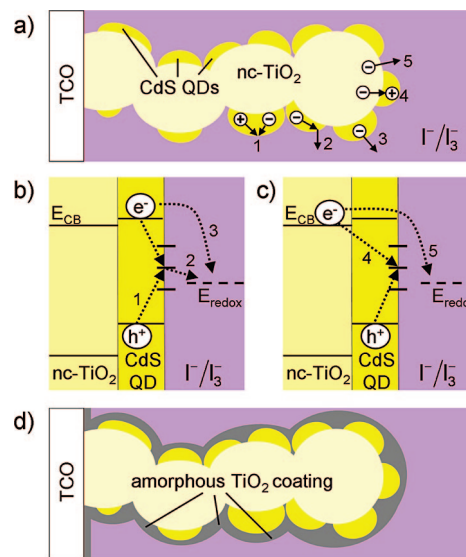


Figure 3. (a) Schematic drawing of the uncoated CdS sensitized nanocrystalline (nc) TiO₂ electrode showing five different recombination paths. (b) Energy band diagram showing the recombination paths of an excited electron in the CdS quantum dot, which can get trapped in a surface state and recombine with the hole (1) or be captured by the oxidized species of the redox electrolyte (2). Furthermore the excited electron can directly be captured by iodine molecules (3). (c) Recombination of electrons from the nc-TiO₂ with a hole trapped in a CdS surface state (4) or direct recombination into the electrolyte through areas which are not covered with CdS (5). (d) Schematic drawing of the CdS sensitized mesoporous TiO₂ electrode with amorphous TiO₂ coating, which blocks and passivates all five recombination paths.

with the electrolyte, often leads to complete dissolution of the QDs into the solution.²⁷ Blocking trap states in which holes can accumulate with an amorphous TiO₂ coating prevents the degradation of the QDs and decreases recombination, resulting in a photostable and efficient cell.

Conclusions

We have shown that CdS QD sensitized solar cells passivated with an amorphous TiO₂ shell can exhibit efficiencies up to 1.24% under one sun. The coating enabled the use of the very corrosive I⁻/I₃⁻ electrolyte, resulting in a better solar cell performance compared to other electrolytes commonly used. The amorphous coating improved the photocurrent, photovoltage, fill factor, and photostability compared to noncoated electrodes. This approach opens new possibilities to improve QD sensitized solar cells using different sensitizers.

Acknowledgment. The authors acknowledge the support from the European Union “OrgaPVnet” project.

References and Notes

- O'Regan, B.; Grätzel, M. *Nature* **1991**, *353*, 737.
- Green, M. A.; Emery, K.; Hishikawa, Y.; Warta, W. *Prog. Photovoltaics* **2008**, *16*, 435.
- Chang, C. H.; Lee, Y. L. *Appl. Phys. Lett.* **2007**, *91*, 053503.
- Eychmüller, A.; Hasselbarth, A.; Katsikas, L.; Weller, H. *J. Lumin.* **1991**, *48–9*, 745.
- Hotchandani, S.; Kamat, P. V. *J. Phys. Chem.* **1992**, *96*, 6834.
- Lin, S. C.; Lee, Y. L.; Chang, C. H.; Shen, Y. J.; Yang, Y. M. *Appl. Phys. Lett.* **2007**, *90*, 143517.
- Toyoda, T.; Saikusa, K.; Shen, Q. *Jpn. J. Appl. Phys.* **1999**, *38*, 3185.
- Liu, D.; Kamat, P. V. *J. Phys. Chem.* **1993**, *97*, 10769.
- Nasr, C.; Kamat, P. V.; Hotchandani, S. *J. Electroanal. Chem.* **1997**, *420*, 201.
- Rincon, M. E.; Jimenez, A.; Orihuela, A.; Martinez, G. *Sol. Energy Mat. Sol. Cells* **2001**, *70*, 163.
- Plass, R.; Pelet, S.; Krüger, J.; Grätzel, M.; Bach, U. *J. Phys. Chem. B* **2002**, *106*, 7578.
- Yu, P. R.; Zhu, K.; Norman, A. G.; Ferrere, S.; Frank, A. J.; Nozik, A. J. *J. Phys. Chem. B* **2006**, *110*, 25451.
- Zaban, A.; Micic, O. I.; Gregg, B. A.; Nozik, A. J. *Langmuir* **1998**, *14*, 3153.
- Kongkanand, A.; Tvrdy, K.; Takechi, K.; Kuno, M.; Kamat, P. V. *J. Am. Chem. Soc.* **2008**, *130*, 4007.
- We note that the recently reported efficiency of 4.15% by Peng and co-workers Peng, L. M. *J. Am. Chem. Soc.* **2008**, *130*, 1124. is based on an incorrect data analysis.
- Diguna, L. J.; Shen, Q.; Kobayashi, J.; Toyoda, T. *Appl. Phys. Lett.* **2007**, *91*.
- Niitsoo, O.; Sarkar, S. K.; Pejoux, C.; Rühle, S.; Cahen, D.; Hodes, G. *J. Photochem. Photobiol., A* **2006**, *181*, 306.
- Lee, Y. L.; Huang, B. M.; Chien, H. T. *Chem. Mater.* **2008**, *20*, 6903.
- Hodes, G. *J. Phys. Chem. C* **2008**, .
- Lee, Y.-L.; Chang, C.-H. *J. Power Sources* **2008**, *185*, 584.
- Vogel, R.; Hoyer, P.; Weller, H. *J. Phys. Chem.* **1994**, *98*, 3183.
- Wu, S.; Han, H. W.; Tai, Q. D.; Zhang, J.; Xu, S.; Zhou, C. H.; Yang, Y.; Hu, H.; Chen, B. L.; Sebo, B.; Zhao, X. Z. *Nanotechnology* **2008**, *19*, 215704.
- Grinis, L.; Dor, S.; Ofir, A.; Zaban, A. *J. Photochem. Photobiol., A* **2008**, *198*, 52.
- Gorer, S.; Hodes, G. *J. Phys. Chem.* **1994**, *98*, 5338.
- Nemec, P.; Nemec, I.; Nahalkova, P.; Nemcova, Y.; Trojanek, F.; Maly, P. *Thin Solid Films* **2002**, *403*, 9.
- Grinis, L.; Zaban, A. *J. Photochem. Photobiol., A* **2008**, submitted for publication.
- Lee, H. J.; Yum, J. H.; Leventis, H. C.; Zakeeruddin, S. M.; Haque, S. A.; Chen, P.; Seok, S. I.; Grätzel, M.; Nazeeruddin, M. K. *J. Phys. Chem. C* **2008**, *112*, 11600.
- Robel, I.; Subramanian, V.; Kuno, M.; Kamat, P. V. *J. Am. Chem. Soc.* **2006**, *128*, 2385.
- Eufinger, K.; Poelman, D.; Poelman, H.; De Gryse, R.; Marin, G. B. *Appl. Surf. Sci.* **2007**, *254*, 148.

JP8108682